Numerical studies of side slip and propeller on tips high aspect ratio wing effect on the inductive drag

© O.V. Pavlenko[1,2], E.A. Pigusov[1,2], M.G. Reslan[2], A. Santhosh[2]

[1] Zhukovsky Central Aerohydrodynamic Institute, Zhukovsky, Moscow oblast, Russia
[2] Moscow Institute of Physics and Technology (National Research University), Dolgoprudny, Moscow Region, Russia
E-mail: olga.v.pavlenko@yandex.ru

Received May 11, 2023
Revised August 30, 2023
Accepted October, 30, 2023

The results of a numerical study of the influence of the angle are presented. sliding and operation of the propeller at the end of a high aspect ratio wing at circulation and inductive reactance. Numerical studies of the influence of angle slip (side wind) on the aerodynamic characteristics of the model aircraft with an ultra-high aspect ratio wing with working propellers at the wing tips were carried out using a program based on the solution Reynolds-averaged Navier–Stokes equations. Numerical studies showed that as the sliding angle increases, circulation decreases and inductive reactance of the wing.

Keywords: pulling propeller, high aspect ratio wing, side slip angle, circulation of the wing, inductive drag References.

DOI: 10.61011/TPL.2023.12.57594.88A

For aircraft (LA), which perform a long flight in cruising mode, the actual task is to reduce inductive drag, as it allows to increase the aerodynamic quality of the aircraft and reduce energy costs by reducing the required thrust, thereby increasing the competitiveness of the created aircraft. For such aircraft, an urgent task is to assess the distribution of loads along the wing span, which makes it possible to develop measures to reduce the negative impact of wing deformations during flights in turbulent atmospheres.

This paper presents the results of computational studies of the effect of the change in the slip angle on the streamline of an aircraft with a mechanized wing of extra-large elongation ($\lambda = 23$), at the ends of which nacelles of 0.35 m diameter are installed with pulling twin-blade air propellers (AP) of 0.22 m diameter, rotational speed $N = 15\,000$ rpm (Fig. 1). The propellers have multi-directional rotation in the direction of the fuselage. Calculations are performed at the screw load value

$$B = \frac{T}{q_\infty F} = 0.5,$$

where T — propeller thrust [N], q_∞ — velocity head, F — area swept by blade ends. Propeller thrust coefficient at zero angles of attack and glide $\alpha_t = T/\rho_\infty n^2 D^4 = 0.06$, where ρ_∞ — air density [kg/m^3], n — propeller speed [Hz], D — propeller diameter [m]. Relative propeller wake $\lambda = V_\infty/nD = 0.044$, where V_∞ — incoming flow velocity [m/s]. In addition, a variant without working air propellers was investigated for comparison. The straight wing with a relative thickness profile $c = c/b_a = 15\%$ (where c — maximum wing profile thickness, b_a — average aerodynamic wing chord, which in this case is equal to the wing chord $b_a = b = 0.106$ m) is equipped with a simple rotary flap and a two-section aileron. The aileron chord is 17% of the wing chord.

Numerical investigations were performed using ANSYS FLUENT program, based on the solution of Reynolds-averaged Navier – Stokes equations, on a structured computational grid. The modelling domain is a parallelepiped of height $57b$ and length $113b$. When modelling in the boundary layer region, the height of the first grid cell near the wing surface was chosen such that the boundary layer could accommodate a sufficient number of cells to calculate the near-wall function and the value of the parameter y^+ in the first near-wall node did not exceed unity (in these calculations with the propeller $y^+ \leqslant 0.82$). A realizable $k-\varepsilon$ turbulence model with improved modelling of turbulence parameters near the wall and taking into account the influence of pressure gradient and compressibility effects is used in the calculation. This turbulence model allows us to make fairly accurate predictions of boundary layer characteristics for large pressure gradients, breakaway and rotating currents [1]. A one-parameter turbulence model adapted to flows with low Reynolds numbers is used in the particle region. In addition, the realizable $k-\varepsilon$ turbulence model is suitable for calculations on a coarse mesh with a small number of cells. A comparison of computational and experimental data is presented in [2,3], and information on propeller thrust is given in [4]. Modelling of the translational motion of the wing and the rotation of the propeller was specified using two computational zones: one — with translational airflow and the other — with rotational airflow modelling the rotation of the propeller. The calculations have been made according to the previously developed method [5]. The grid independence data of the computational model without AP are presented in the table. As a result, a grid with 20 million cells was chosen as the base grid.

Calculations have been carried out at angle of attack $\alpha = 0$ in the range of glide angles β from 0 to 20°

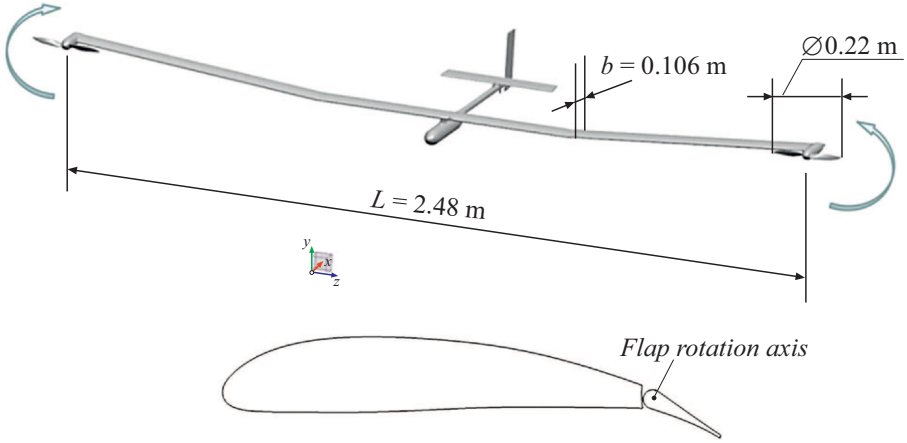

Figure 1. Computational model of an aircraft and wing profile with deflected $\delta_{mech} = 15°$ mechanization.

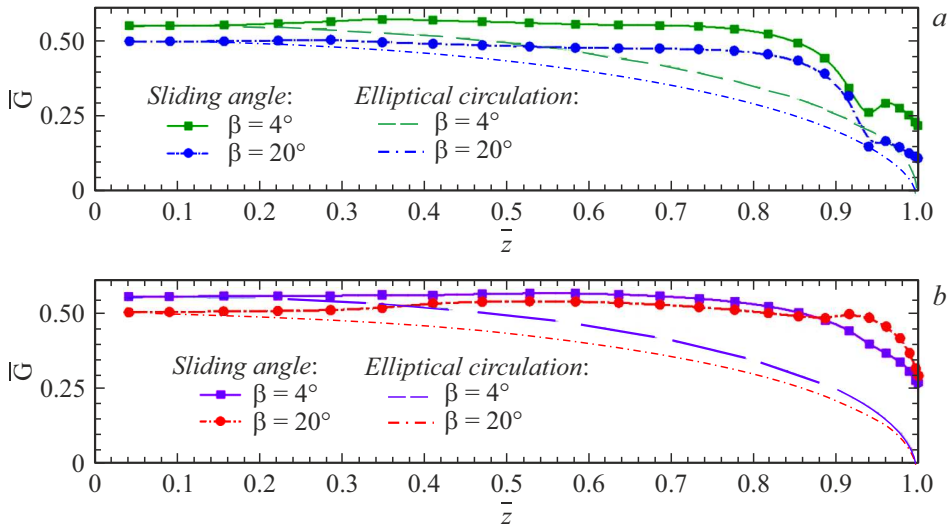

Figure 2. Influence of slip angle on the wingspan circulation of an AP blown wing ($\alpha = 0$). *a* — left wing cantilever, *b* — right wing cantilever.

at an incoming flow velocity $V_\infty = 50$ m/s and Reynolds number $\mathrm{Re} = 0.35 \cdot 10^6$ with deflected wing mechanization $\delta_{mech} = 15°$, corresponding to its take-off position.

It is known that the minimum inductive drag is achieved on a straight wing with an elliptical circulation distribution along the sweep. The effect of BB on the relative circulation over the wingspan, which was calculated by the formula

$$\bar{G} = \frac{G\pi L}{2V_\infty S C_l}$$

(where $G = C_{l\,sect} b_a V_\infty / 2$, C_l — wing lift coefficient, $C_{l\,sect}$ — wing section lift coefficient, L — wing span [m], S — wing area [m^2]), shown in Fig. 2. For comparison, the figure shows the elliptical circulation over the wing span plotted for each glide angle using the ellipse formula and having minimum inductive drag:

$$C_{xa} = \frac{1}{\pi \lambda_w} C_l^2,$$

Aerodynamic coefficients of the model without AP ($\alpha = 0, \beta = 0$)

Number of grid cells	C_y	C_x
10 mln	0.8112	0.0635
20 mln	0.8081	0.0573
26 mln	0.8072	0.0586

where λ_w — wing elongation. Increasing the glide angle β from 0 to 20° and air propeller blowing mainly affect the circulation of the left leeward wing cantilever. On the right windward wing cantilever, the decrease in circulation with increasing glide angle occurs only locally in the propeller jet blowing area. The circulation values obtained from the modelling are different from zero at the wing tip due to the presence of the nacelle, which has its own lift force.

In accordance with the Prandtl finite span wing theory, the minimum inductive drag corresponds to an elliptical distribution of circulation over the wing span. In this

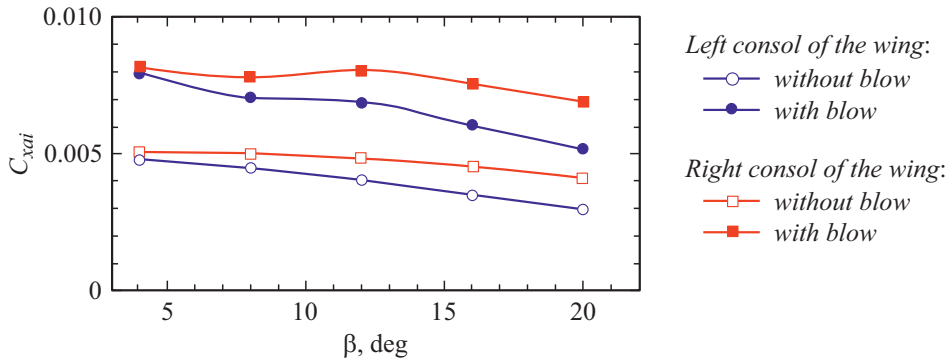

Figure 3. The value of the inductive resistance coefficient as a function of the slip angle ($\alpha = 0$).

case, the inductive drag coefficient of the wing C_{xai} varies inversely with the geometric elongation of the wing

$$C_{xai} = \frac{1}{\pi\lambda} C_{ya}^2,$$

where C_{ya} — the lift coefficient. In practical applications, this is accounted for approximated by introducing a correction factor for straight wings $\delta = 0.05$ into the design formula for the inductive drag coefficient. Thus, the inductive drag coefficient in the present work was calculated using the formula

$$C_{xai} = \frac{1+\delta}{\pi\lambda} C_{ya}^2.$$

. Increasing the slip angle decreases the circulation over the wing span and brings it closer to an elliptical shape. Therefore, the lowest inductive resistance is observed at large slip angles (Fig. 3). As the slip angle increases, a decrease in inductive resistance is observed both with and without operating propellers. It should be noted that in the large slip angle range ($12 \leqslant \beta \leqslant 20°$), the derivative of the inductive drag coefficient function over the slip angle C_{xai}^{β} is higher with operating air screws than without them. But increasing the glide angle β affects the inductive drag of the wing cantilevers differently. For example, the inductive resistance of the right windward wing cantilever is noticeably greater than that of the left. And this difference only increases with increasing slip angle β. For example, at slip angle $\beta = 4°$, the inductive drag for the right windward wing cantilever is 1.1 times and at $\beta = 20°$ 1.4 times that for the left wing cantilever. At slip angle $\beta = 20°$, the inductive drag of the right windward wing cantilever with the propellers operating at its ends is about 1.7 times greater than without them.

Numerical investigations of the streamline of a model aircraft with a wing of large elongation and deflected wing mechanization $\delta_{mech} = 15°$, corresponding to its take-off position, have shown that an increase in the slip angle reduces the wing lift force (decreasing the circulation over the wing span) and consequently the inductive drag, especially in the case of operating propellers.

Conflict of interest

The authors declare that they have no conflict of interest.

References

[1] T.-H. Shih, W.W. Liou, A. Shabbir, Z. Yang, J. Zhu, Comput. Fluids, **24** (3), 227 (1995). DOI: 10.1016/0045-7930(94)00032-T
[2] O.N. Vinogradov, A.V. Kornushenko, O.V. Pavlenko, A.V. Petrov, E.A. Pigusov, T.N. Chin, Vestn. MAI, **28** (2), 7 (2021). DOI: 10.34759/vst-2021-2-7-19
[3] O.V. Pavlenko, G.R. Reslan, Vestn. MAI, **29** (3), 17 (2022). DOI: 10.34759/vst-2022-3-17-28
[4] O.N. Vinogradov, A.V. Kornushenko, O.V. Pavlenko, A.V. Petrov, E.A. Pigusov, T.T. Ngoc, J. Phys.: Conf. Ser., **1959**, 012051 (2021). DOI: 10.1088/1742-6596/1959/1/012051
[5] V.S. Alesin, V.V. Gubsky, O.V. Druzhinin, V.Y. Yeremin, O.V. Pavlenko, Avtomatizatsiya. Sovremennye tekhnologii, **72** (2), 91 (2018). (in Russian).

Translated by J.Deineka